1 Supporting Information

Sample compositions

The soybean phosphatidylcholine (SPC) grade employed, Lipoid S100, has a purity of $>94\%w$ phosphatidylcholine (PC) with fatty acid composition of 59% C18:2 (linoleic), 12 % C16:0 (palmitic) and 7% C18:1 (oleic) (other fatty acids being minor contributors).

Table SI 1: Compositions of the lipid formulations used for the present study. Liposomes were extruded at room temperature (RT) as transition temperature (T_m) of SPC is $\leq$ -15 °C and so RT$>T_m$.

SPC ($\%w$)	LPC ($\%w$)	SPC:LPC
0.5 %	0 %	100:0
	0.01 %	98:2
	0.02 %	96:4
	0.05 %	91:9

Light scattering

The intensity autocorrelation functions ($g^{(2)}$) obtained by dynamic light scattering (DLS) were evaluated with the cumulant analysis, from which diffusion coefficients (D) are obtained. The hydrodynamic radius (R_h) was calculated from the Stokes-Einstein relation $R_h = k_B T/6\pi\eta D$ where k_B is the Boltzmann constant and η the solvent viscosity.

Static light scattering (SLS) experiments were performed in the same instrument used for DLS. Data at low-q from SLS experiments was fitted using the Guinier approximation [1] (Equation (SI 1)) valid for $qR_g \ll 1$ to obtain the radius of gyration (R_g) and forward scattering $I(0)$.

$$I(q) = I_0 P(q) \approx I_0 \exp\left(-\frac{q^2 \langle R_g \rangle^2}{3}\right) \quad \text{(SI 1)}$$

The mass-average molecular weight of the liposomes was obtained from I_0 with the relation

$$MW_{liposome} = \frac{I_0}{Kc}, \quad \text{(SI 2)}$$

where K is the optical constant $K = (4\pi^2 n_s^2 (dn/dc)^2)/(\lambda^4 N_a)$, c the mass concentration, N_a Avogadro's constant and dn/dc the refractive index increment, calculated as 0.160 mL/g from the difference between the refractive index of water and phospholidpids, 1.332 and 1.493, respectively, divided by the lipid density ($\sim$1 g/mL [2]).

$MW_{liposome}$ can be compared to the expected molecular weight of a unilamellar vesicle (MW_{ULV}) to derive the lamellarity of the liposome. MW_{ULV} is calculated by

$$MW_{ULV} = \frac{N_A}{\nu}\frac{4\pi}{3}\left(R^3 - (R-\delta)^3\right), \quad \text{(SI 3)}$$

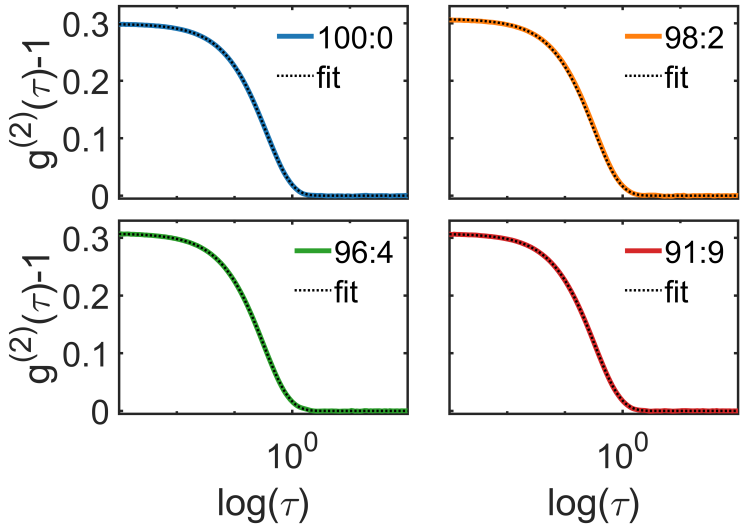

Figure SI 1: DLS data of SPC:LPC extruded liposomes and respective fits done with the cumulant analysis.

where R is the outer radius of the vesicle obtained from DLS and δ the bilayer thickness.

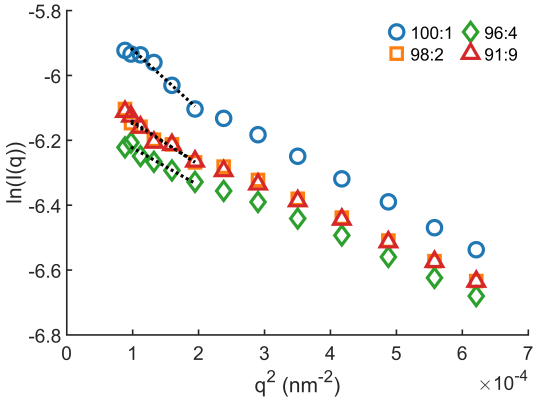

Figure SI 2: SLS data of SPC:LPC extruded liposomes. Dashed black lines represent the Guinier fits.

Small-Angle Neutron Scattering

Due to the limited experimentally accessible q-range, extrapolation to $q \rightarrow 0$ and $q \rightarrow \infty$ is necessary to derivate the scattering invariant from experimental SANS curves.

The invariant is therefore partitioned in 3 components as described by Equation (SI 4), the second term being the experimentally available information.

$$Q_{inv} = \int_0^{q_{min}} q^2 I_{Guinier} + \int_{q_{min}}^{q_{max}} q^2 I(q) dq + \int_{q_{max}}^{\infty} q^2 I_{Porod} \tag{SI 4}$$

Extrapolation of the scattered intensity to q = 0 was done by fitting within the Guinier region (low-q region), where $I(q)$ should vary according to Equation (SI 1). By doing so, the value of $I_{Guinier}$ was obtained and it constitutes approximately 2.4 % of the Q_{inv} of our systems.

The third component of Equation (SI 4) refers to the Porod regime, where it is assumed that scattering contributions derive from reflections of sharp interfaces as there is no shape information left of the system at very high q-values, when $qR \gg 1$. In this region, scattering follows the Porod law where the power law exponent is fixed to 4 and the scattered intensity is described by Equation (SI 5)[3]

$$I(q) = \frac{1}{q^4} 2\pi (\Delta SLD)^2 S_v + I_{background}, \tag{SI 5}$$

where S_V is the specific surface area. For our systems, the Porod region accounts for 3 % to 8 % of our calculated Q_{inv}. See Figure SI 4 for examples of the Guinier and Porod extrapolations.

For a system with two components and sharp interfaces the scattering invariant is directly linked to the volume fractions of the components

$$Q_{inv} = 2\pi^2 \phi_1 \phi_2 \Delta SLD^2, \tag{SI 6}$$

where ϕ_i is the volume fraction of component i and ΔSLD is the scattering length density difference between the two components.

Here, we treat our dispersions as a two component system, made of liposomes composed of double and single chain phospholipids (soybean and lysophosphatidylcholine, SPC and LPC, respectively) and solvent. At concentrations of the LPC below bilayer solubilization, all lipids are assumed to reside in the liposome phase and a fraction of water can penetrate into the lipid bilayer while the remainder forms the solvent phase, so that the volume fraction of the liposomes is given by

$$\phi_1 = \phi_{SPC} + \phi_{LPC} + \beta \phi_{wat} \tag{SI 7}$$

and the volume fraction of the solvent phase is given by

$$\phi_2 = (1 - \beta) \phi_{wat}, \tag{SI 8}$$

where β is the fraction of water contained in the liposome membranes. As a consequence, the *SLD* of the liposomes reads

$$SLD_1 = \left[\frac{1}{\phi_1} \right] \left[\phi_{SPC} SLD_{SPC} + \phi_{LPC} SLD_{LPC} + \beta \phi_{wat} SLD_{wat} \right], \tag{SI 9}$$

whereas the solvent *SLD* will be that of heavy water (SLD_{wat}).

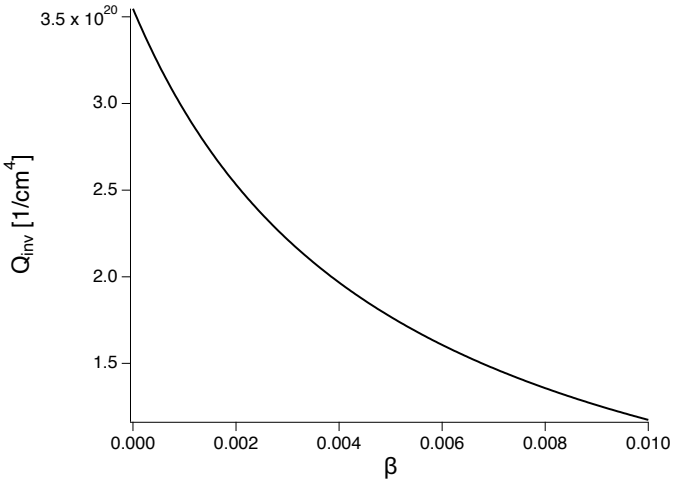

Figure SI 3: Calculated invariant for lipid solution with volume fraction $\phi_{PC} = 0.005$, $SLD_{PC} = 0.32E10$ 1/cm^2 in heavy water ($SLD_{solv} = 6.33E10$ 1/cm^2) as a function of the level of solvent incorporation in the membrane β according to eqs. (2) to (5); the invariant decreases with an increasing amount of incorporated solvent.

Substitution of Equations SI 7-SI 9 in Equation (SI 6) and simplification of the expression lead to:

$$Q_{inv} = 2\pi^2 \phi_1 \phi_2 \left(\frac{\phi_{SPC}(SLD_{SPC} - SLD_{wat}) + \phi_{LPC}(SLD_{LPC} - SLD_{wat})}{\phi_{SPC} + \phi_{LPC} + \beta\,\phi_{wat}} \right)^2, \quad \text{(SI 10)}$$

and the simplified expression after expansion of the binome reads

$$Q_{inv} = 2\pi^2 (1-\beta)\,\phi_{wat} \frac{\phi_{SPC}^2 A^2 + \phi_{LPC}^2 B^2 + 2\phi_{SPC}\phi_{LPC} AB}{\phi_{SPC} + \phi_{LPC} + \beta\,\phi_{wat}}, \quad \text{(SI 11)}$$

where $A = SLD_{SPC} - SLD_{wat}$ and $B = SLD_{LPC} - SLD_{wat}$.

Considering that $\phi_{SPC}^2 A^2 + \phi_{LPC}^2 B^2 + 2\phi_{SPC}\phi_{LPC} AB$ is a constant, K, Equation (SI 11) reads

$$Q_{inv} = \frac{2\pi^2 (1-\beta)\,\phi_{wat} K}{\phi_{SPC} + \phi_{LPC} + \beta\,\phi_{wat}}. \quad \text{(SI 12)}$$

In the event where water was to penetrate the membrane of the liposomes, then $\beta > 0$, resulting in an overall decrease of Q_{inv} as deducted from Equation (SI 12). Finally, the solution for β from eq. (SI 12) is:

$$\beta = \frac{2\pi^2 \phi_{wat} K - Q_{inv}(\phi_{SPC} + \phi_{LPC})}{\phi_{wat} Q_{inv} + 2\pi^2 \phi_{wat} K}. \quad \text{(SI 13)}$$

Table SI 2: Parameters used to calculate the expected values of the scattering invariant Q_{inv}^{theo} by mass balance . For SPC, a scattering length density of 0.32×10^{10} cm^{-2} based on an average composition $C_{42}H_{80}NO_8P$ and a density of 1.01 g/cm^3 were assumed. The employed SLD and density values for LPC were 0.39×10^{10} cm^{-2} and 1.08 g/mL, respectively. LPC density was calculated assuming a lipid volume of $\sim$800 Å^3 and considering that a PC headgroup is about $\sim$300 Å^3 and the DOPC volume is $\sim$1300 Å^3 [4].
Finally, the SLD value of the solvent was that of heavy water, 6.3×10^{10} cm^{-2}

SPC:LPC	$\phi_{SPC}\times10^{-3}$	$\phi_{LPC}\times10^{-3}$	$SLD_{lipids}\times10^{10}$ (cm^{-2})	$Q_{inv}^{theo}\times10^{20}$ (cm^{-4})
100:0	5.4	0	0.328	3.790
98:2	5.4	0.102	0.329	3.860
96:4	5.4	0.204	0.330	3.929
91:9	5.4	0.509	0.333	4.138

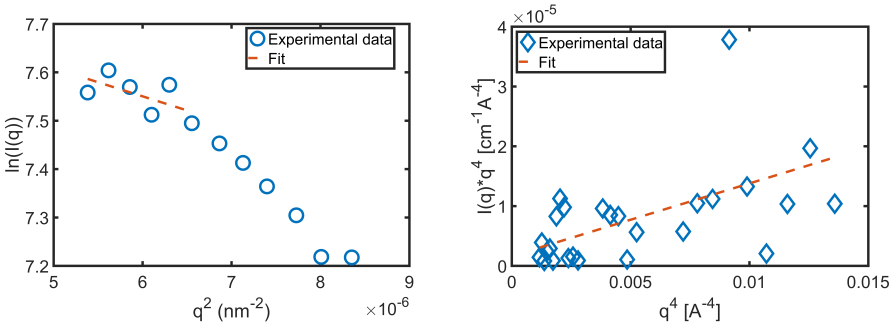

Figure SI 4: Example of fits within the Guinier (Figure SI 4a) and Porod (Figure SI 4b) regions of a SANS curve. The experimental data corresponds to extruded soybean phosphatidylcholine (SPC) liposomes (0.5%) in D_2O.

Table SI 3: Detailed summary of the parameters obtained from the model-free analysis of SANS curves of SPC:LPC liposomes. The experimental scattering invariants (Q_{inv}) were obtained by summing the contributions from the experimental data Q_{inv}^{exp} and from the extrapolations in the Guinier and Porod regions ($Q_{inv}^{Guinier}$ and Q_{inv}^{Porod}, respectively)

SPC:LPC	$Q_{inv}^{theo}\times10^{20}$ (cm^{-4})	$Q_{inv}^{Guinier}\times10^{20}$ (cm^{-4})	$Q_{inv}^{exp}\times10^{20}$ (cm^{-4})	$Q_{inv}^{Porod}\times10^{20}$ (cm^{-4})	$Q_{inv}\times10^{20}$ (cm^{-4})
100:0	3.788	0.104	3.500	0.057	3.662
98:2	3.862	0.080	2.726	0.268	3.075
96:4	3.936	0.084	3.033	0.122	3.240
91:9	4.157	0.069	3.220	0.214	3.504

The appearance of pores can be explained as follows: at low concentrations, the lysolipid should be incorporated into the lipid bilayer and the inverted cone structure

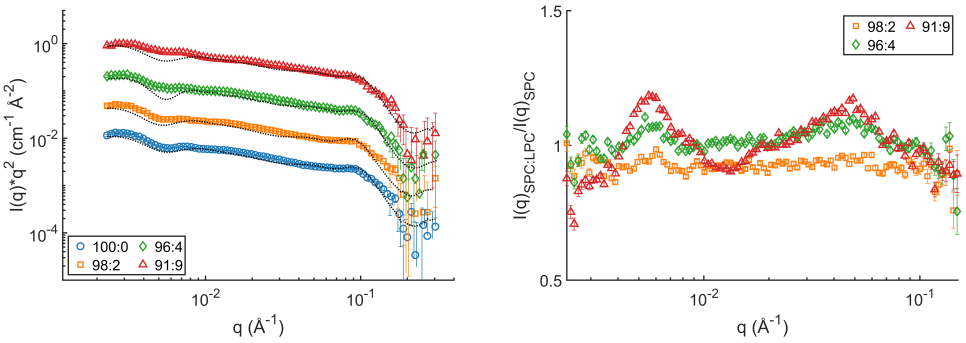

(a) (b)

Figure SI 5: Results of SANS experiments on SPC:LPC liposomes extruded with a 100 nm pore size membrane. (SI 5a) Experimental data represented as Kratky plots ($I(q)q^2$ vs. q) at different SPC:LPC ratios and corresponding fits using a combination of form factors accounting ULV and MLVs. (SI 5b) shows the scattered intensity of SPC:LPC vesicles normalized over that of SPC liposomes to highlight changes in I(q). At increasing LPC content, liposomes become more polydisperse as observed from the smearing out of the form factor minima.

of LPC would promote positive curvature of the membrane[32,38]. Further addition of surfactant should create LPC enriched regions with a localized high curvature. This structural feature should foster the formation of pores or domains of high curvature to prevent exposure of the hydrophobic bilayer core to water. Past a critical SPC:LPC ratio, the membrane will no longer be able to accomodate more surfactant and beyond this critical point, further LPC will assemble in form of micelles.[40].

In the case where vesicles and micelles were to co-exist in a dispersion, the SANS experiments performed in this work would not allow to corroborate the presence of the formed micelles. Their scattering signal would be overshadowed by that of the liposomes, as SANS modelling shown in Figure SI 6 suggests.

Table SI 4: Parameters employed for fitting SANS curves presented in Figure (4) Figure 3 with the contributions of unilamellar (U) and multilamellar (M) vesicle models. The contrast factors ($SLDs$) and total volume fractions ($\phi_U + \phi_M$) were obtained from the analysis of the scattering invariant. Liposome radius (R_g) was obtained from SLS investigations presented in Table 1.

SPC:LPC	SLD_{solv} $\times 10^{10}$ (cm^{-2})	SLD_{lipo} $\times 10^{10}$ (cm^{-2})	ϕ_U ($\%v$)	$R_{U,o}$ (nm)	δ_U (nm)	ϕ_{MLV} ($\%v$)	$R_{M,i}$ (nm)	δ_M (nm)	$\delta_M^{H_2O}$ (nm)	N_M
100:0	6.33	0.52	0.4	57.7	2.9	0.16	39.1	2.9	2.0	3
98:2	6.33	1.54	0.5	58.7	2.9	0.21	42.0	2.9	2.0	3
96:4	6.33	1.38	0.5	56.0	2.9	0.18	38.0	2.9	2.0	3
91:9	6.33	1.26	0.53	55.0	2.9	0.18	40.3	2.9	2.5	3

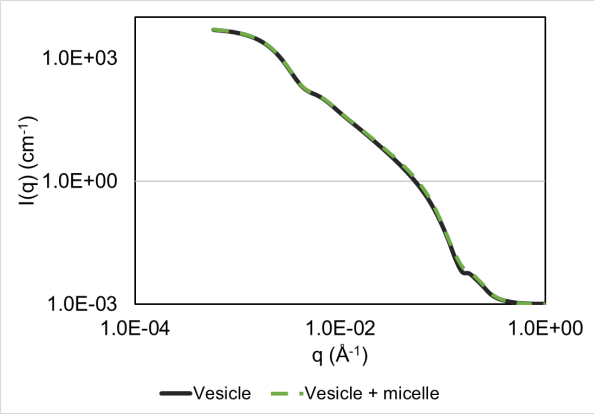

Figure SI 6: Modelled SANS curves of unilamellar vesicles ($\phi = 0.5$, R = 60 nm, δ = 3.9 nm) and ULVs in the presence of micelles wih volume fraction $\phi = 0.05$ and radius of 4 nm. The volume fraction of micelles corresponds to the highest concentration of LPC added to the dispersion. The assumed contrast was $SLD_{PC} = 0.32E10$ 1/cm^2 and heavy water $SLD_{solv} = 6.33E10$ $1/\text{cm}^2$.

Hydration number

Knowing the densitites of the components, the volume fraction of hydrating water molecules in the lipid bilayer ($\phi_{D_2O}^{lipo}$) obtained from the analysis of the invariant can be converted into mass fraction ($x_{N,D2O}$). Density of the vesicles was derived from the specific volume of 0.9848 cm^3/g[5].

Thereafter, the number of hydrating water molecules per lipid molecule (N_{D_2O}) can be calculated from the relation Equation (SI 14),

$$N_{D_2O} = \frac{x_{N,D_2O} x_{solvent} \rho_{D_2O}}{[N_{lipids}]} \frac{N_A}{MW_{D_2O}}, \tag{SI 14}$$

with $x_{solvent}$ the mass fraction of all the solvent, ρ the density of heavy water (1.1 =g/mL at 25 °C), N_A is the Avogadro constant, MW the molecular weight, and $[N_{lipids}]$ is the number of lipid molecules per liter estimated as:

$$[N_{lipids}] = c_{lipids} * MW_{lipids}^{-1} * N_A, \tag{SI 15}$$

where c_{lipids} is the mass concentration of the lipids.

Pore density

Assuming that all LPC molecules partake in the stabilization of pores, then Equation (SI 16) is used to obtain the ratio between V_{pores}/A_{LPC}. Values for the constants are $MW_{LPC} = 521$ g/mol, $\hat{V}_{LPC} = 0.9246$ mL/g assuming a lipid volume of 800 Å^3 as described in Table SI 2, A_{LPC} as 70 Å^2 [6] and N_A as Avogadro's constant.

$$\frac{V_{pores}}{A_{LPC}^{pores}} = \frac{V_{pores}}{V_{lyso}^{lipo}} \frac{MW_{LPC} \hat{V}_{PL}}{N_A A_{LPC}}. \tag{SI 16}$$

Converting to the appropriate units, a pore volume over LPC area ratio of 12.42 nm is calculated from Equation (SI 16). As mentioned in the main text, the V/A relation is key as it can be related to geometrical structures that the pore and the LPC belt can have. In addition, it allows for the estimation of a pore radius, necessary to estimate ρ_{pore}.

The pore volume is assumed to be related to that of a cylinder ($V_{cyl} = \pi r^2 \delta$) and the area of the lysolipids can be related to the lateral surface of that same cylinder by

$$A_{cyl}^{lat} = 2\pi r \delta, \tag{SI 17}$$

where δ is the bilayer thickness considered to be 3.9 nm. Assuming the shape of a cylinder, the relation V/A reads

$$\frac{V_{cyl}}{A_{cyl}^{lat}} = \frac{\pi r^2 h}{\pi r h} 2 = r_{pore}. \tag{SI 18}$$

The second option is to consider A_{LPC}^{pores} as the surface area of the inner part of a torus using Equation (SI 19) whilst assuming the volume of a cylinder for V_{pores} to find the lower limit of r_{pore}. Resulting values are reported in Table SI 5.

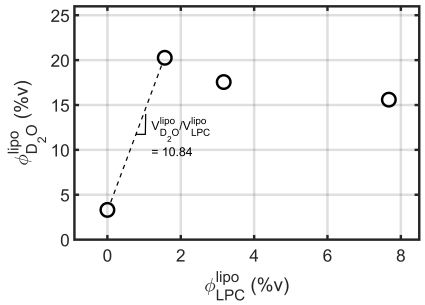

Figure SI 7: Calculated volume fractions of D_2O incorporated to the SPC liposomes vs. volume fraction of LPC, both with respect to the liposome phase. $\phi^{lipo}_{D_2O}$ calculated from model-free analysis of SANS curves.

Table SI 5: Geometric structures considered for A^{pores}_{LPC}

Geometry for A_{LPC}	r_{pore} (nm)
Cylinder (lateral A)	26.65
Torus (inner A)	21.45

Figure SI 7 is the starting point to calculate the pore density (ρ) in nm^{-2}. Assuming that $\phi^{lipo}_{D_2O}$ corresponds to the volume fraction of pores in the liposomes, then the relation $V^{lipo}_{D_2O}/V^{lipo}_{lyso} = V_{pores}/V^{lipo}_{lyso} = 10.8$ is obtained from the $\phi^{lipo}_{D_2O}$ vs. ϕ^{lipo}_{LPC} plot.

$$A^{inner}_{torus} = 2\pi\,(r+\delta/2-\delta/\pi)\,(\pi\delta/2) \tag{SI 19}$$

In order to calculate the pore density, it is assumed that in a 2D representation there will be one pore (or the equivalent of a circle) per square of a certain length L. That way, the areas are related to $\phi^{lipo}_{D_2O}$ as follows

$$\phi^{lipo}_{D_2O} = \frac{A_{pore}}{A_{square}} = \frac{\pi r^2_{pore}}{L^2}. \tag{SI 20}$$

Equation (SI 20) is solved for L, from which δ_{pore} is calculated as there will be one pore per square of area L^2, equally described by

$$\rho_{pore} = \frac{1\text{ pore}}{L^2}. \tag{SI 21}$$

References

[1] A. Guinier and G. Fournet, *Small-Angle Scattering of X-rays*, John Wiley & Sons, 1955.

[2] J. H. Van Zanten and H. G. Monbouquette, *J. Colloid Interf. Sci.*, 1991, **146**, 330–336.

[3] G. Porod, *Kolloid-Zeitschrift*, 1951, **124**, 83–113.

[4] J. F. Nagle, R. M. Venable, E. Maroclo-Kemmerling, S. Tristram-Nagle, P. E. Harper and R. W. Pastor, *J. Phys. Chem. B*, 2019, **123**, 2697–2709.

[5] G. C. Newman and C.-H. Huang, *Biochemistry*, 1975, **14**, 3363–3370.

[6] J. F. Nagle and S. Tristram-Nagle, *BBA-Biomembranes*, 2000, **1469**, 159–195.